



RESEARCH ARTICLE

Adsorption study of mango peel activated carbon as iron removal for batik waste industry

Agung Nugroho^{1,*}, Nur Layli Amanah², Revo Gilang Firdaus¹

¹Department of Chemical Engineering, Universitas Pertamina, Jl. Teuku Nyak Arief, Simprug, Kebayoran Lama, Jakarta 12220, Indonesia

²Department of Materials Science and Engineering, National Taiwan University of Science and Technology, Taipei 10672, Taiwan

Received 27 September 2021; revised 8 November 2021; accepted 12 January 2022



OBJECTIVES The purpose of this study was to determine the optimum process variation in absorbing heavy metal ion Fe contained in batik waste. **METHODS** Four variation methods of activated carbon synthesis were explored to determine the most suitable method of AC synthesis. **RESULTS** FTIR showed that the functional groups in mango peel were visible for all variations of the process, namely hydroxyl (-OH) derived from cellulose and hemicellulose and carboxyl (-COOH) derived from pectin. The adsorption study showed that the most suitable isotherm for all process variations was Langmuir with an R^2 value of 0.9999 for the MPAC-4 sample. The adsorption mechanism is physisorption with a value of $E < 8$ kJ/mol based on the D-R isotherm and has the largest adsorption capacity of $Q_{\max} = 8.2$ mg/g. **CONCLUSIONS** The results showed that the sample synthesized using a combination physical-chemical-physical process was the best process variation resulting in percentage removal of Fe^{2+} of 84.81%.

KEYWORDS batik waste; adsorption; activated carbon; iron waste; mango peel

1. INTRODUCTION

Currently, the batik industry in Indonesia has grown very rapidly. Various household-scale businesses (home industry) and even large-scale businesses continue to grow. On the other hand, the waste generated from the batik-making process also has an impact on the environment. The batik li-

quid waste will be carried away by water in the manufacturing process. There are four steps in the batik-making process, namely mordanting, coloring, fixation, and cleaning. These processes use mainly heavy metals precursors such as iron which are carried as dangerous substances in the wastewater stream.

Conventional methods for removing heavy metals from industrial effluents include chemical precipitation, reverse osmosis, electro dialysis, coagulation, etc (Barakat 2011; Gunatilake 2015). Adsorption is one of the most promising methods for heavy metal removal as it offers cost-effectiveness, simplicity, high removal efficiencies, availability of the number of adsorbents, and is environment friendly. Adsorbents such as silica and activated carbon can be used in the heavy metal removal of wastewater (Khan et al. 2020; Sheth et al. 2021). Activated carbon is one of the most efficient adsorbents for the removal of wide variety of contaminants present in the aquatic environment. Utilization of agricultural waste by-products such as sugarcane bagasse (Mohan and Singh 2002), coconut husk (Tan et al. 1993), rice husk (Ajmal et al. 2003), sawdust (Kadirvelu et al. 2003), etc., as a precursor to synthesis activated carbon, have been investigated by various researchers.

In Indonesia, mango is one of the most familiar horticultural commodities because it can be processed in various forms. In the mango processing industry, mango peel (which contributes to 7-24% of total weight) is dumped as waste (Ghosh et al. 2019) This can cause environmental problems especially related to land use for disposal. Mango peel contains many polymer compounds that have functional groups such as pectin and cellulose (Correia et al. 2018). This polymer can increase the possibility of mango peel as a carbon source that can be converted into activated carbon (Ghosh et al. 2019) which can be utilized further to adsorb heavy metal waste such as Fe^{2+} which is large presence in batik industrial waste.

In this research, an adsorption study of Fe^{2+} metal ions dissolved in water was carried out using activated carbon synthesized from mango peel (Budiyanto et al. 2018). Moreover, the adsorption process of mango peel-activated carbon was modeled using the Freundlich, Langmuir, and Dubinin-

*Correspondence: agung.n@universitaspertamina.ac.id

TABLE 1. Variation of the activation process and the resulting yield.

No.	Sample name	Activation process	Yield (%)
1	MPAC-1	Physical (700°C, 1 h)	24.5
2	MPAC-2	Chemical (immersed in H ₂ SO ₄ 1 M for 24 h) - Physical (700°C, 1 h)	31.4
3	MPAC-3	Chemical (immersed in H ₂ SO ₄ 1 M for 24 h) - Physical (300°C, 1 h)	62.8
4	MPAC-4	Physical (300°C, 0.5 h) - Chemical (immersed in H ₂ SO ₄ 1 M for 24 h) - Physical (700°C, 0.5 h)	40.5

Radushkevich isotherm method to determine the adsorption mechanism that occurred. The parameters used in this study were process variations and variations in the concentration of Fe²⁺ metal ions and batik waste. The sample solution was analyzed using the Atomic Absorption Spectroscopy (AAS) to determine the amount of Fe²⁺ ions in the solution before and after adsorption. Meanwhile, the activated carbon samples will be analyzed using FTIR to identify the functional groups of activated carbon.

2. RESEARCH METHODOLOGY

2.1 Activated carbon raw materials

Many required materials to produce MPAC, which covers mango peels as a base material, adsorbates Fe²⁺ ion which derives from FeSO₄ crystals as a model solution and distilled water for all solutions. On another side, H₂SO₄ is used for immersed some samples in Table 1. Also, argon is a gas atmosphere used during the heating process.

2.2 Adsorbate (Fe²⁺s)

Fe²⁺ ion used as model solution which derives from FeSO₄ crystals and also using the distilled water to prepare all solutions Fe²⁺. FeSO₄ crystals were dissolved in distilled water to make water samples with concentrations of 2, 4, and 6 ppm of Fe²⁺. As a comparison, wastewater of the batik home industry from Pekalongan, Central Java was analyzed by Atomic Absorption Spectroscopy (AAS) to determine its Fe²⁺ content.

2.3 Preparation of activated carbon

Mango peel, as the raw material, is dried at 100°C for 24 hours. Before the activation procedure, dried mango peel is grounded and sieved to get the uniform size to 100 mesh. Process variation is carried out by utilizing the combination of physical and chemical activation based on Table 1. For the physical process, the heating rate is 10°C per minute. While chemical activation is done by immersing the sample in 1M H₂SO₄ solution and stirring for 24 hours. After the physical and or chemical activation, the sample was dried for 1 hour at a temperature of 100°C.

2.4 Batch adsorption experiment

A total of 40 mL of adsorbate with a concentration of 2 ppm, 4 ppm, 6 ppm, and batik waste were contacted with each adsorbent. Each sample was put into the incubator shaker at a speed of 150 rpm for 2 hours at room temperature. After the contacting process is complete, filtering is done using a vacuum filtration system. The obtained filtrate was analyzed using AAS to determine the final concentration of Fe (C_e). The final concentration obtained will be used to determine the removal percentage and maximum adsorption capacity.

The amount of Fe concentration absorbed by activated carbon (adsorbent) per initial Fe concentration can be calculated using Equation 1.

$$\% \text{Removal} = \frac{(C_o - C_e)}{C_o} \times 100\% \quad (1)$$

where C_o is the initial concentration of Fe²⁺ ions in solution and C_e is the final concentration of Fe²⁺ ions in solution.

The maximum adsorption capacity of an adsorbent at a certain adsorbent volume and mass can be calculated using Equation 2.

$$q_e = \frac{(C_o - C_e) V}{W} \quad (2)$$

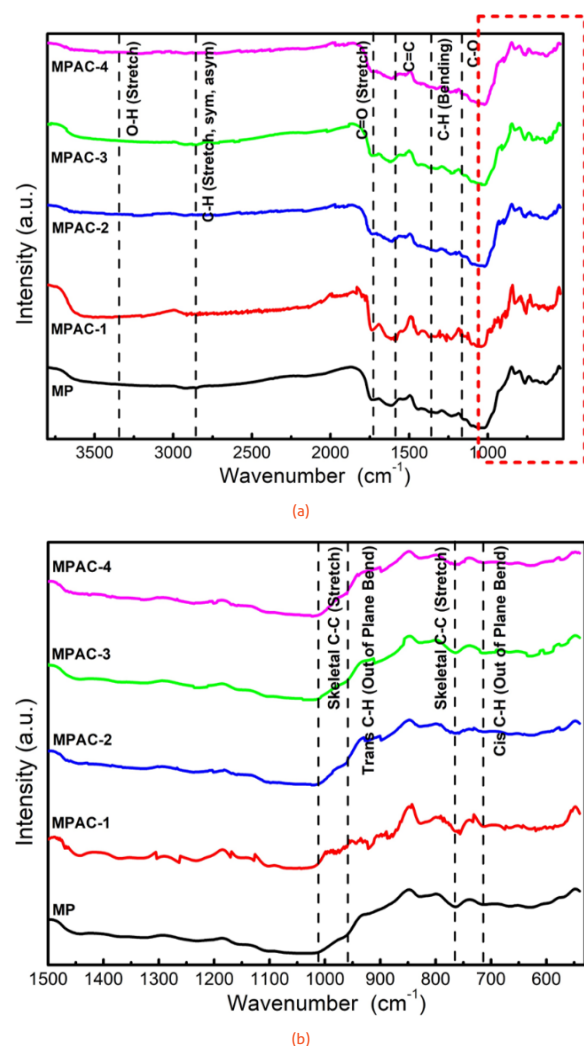


FIGURE 1. FTIR spectrum of MP, MPAC-1, MPAC-2, MPAC-3, and MPAC-4. (a) Full spectrum and (b) zoom view of 500–1500 cm⁻¹.

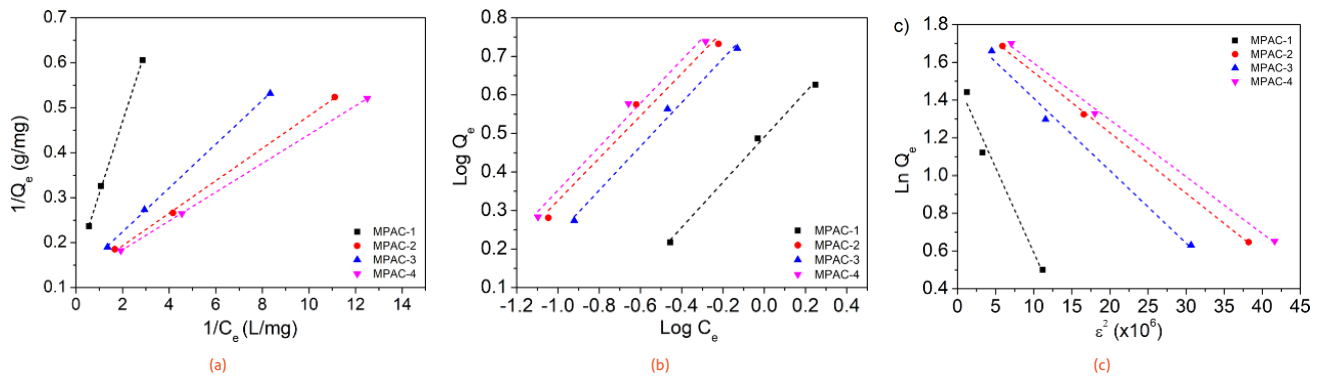


FIGURE 2. Fitting of adsorption isotherm model of Langmuir (a), Freundlich (b), and Dubinin-Radushkevich (c) from the various sample.

where q_e is the maximum adsorption capacity. C_0 is the initial concentration of Fe^{2+} ions in solution, C_e is the final concentration of Fe^{2+} ions in solution, while V is the volume of the solution, and W is the mass of the adsorbent.

2.5 Adsorbent and batik waste characterization

The carbon results from the four process variations were characterized using Fourier Transform Infrared Spectroscopy (FTIR, Nicolet iS5) with the KBr pellet method to know the functional group contained in each sample. While Atomic Absorption Spectroscopy (AAS, NovAA 300) was used to determine the Fe^{2+} concentration before and after the adsorption process.

3. RESULTS AND DISCUSSION

3.1 Activation of mango peel

Mango peel that has been dried and mashed, undergoes activation of various combination processes as shown in Table 1. All four variations of the process produce a black and dry adsorbent. Orozco et al. (2014) mention that during the activation process of fruit waste, there was a decomposition of pectin at $172^\circ C$, hemicellulose at $180-270^\circ C$, and cellulose at $270-370^\circ C$, and lignin at $385-585^\circ C$ (Orozco et al. 2014). Thus, activation at $700^\circ C$ will result in a lower carbon yield compared with activation at other lower temperatures. From the four variations of the process, it turns out that there is no ash formation due to the use of argon gas atmosphere during heating from a temperature of $200^\circ C$. The use of argon

is carried out to avoid the presence of oxygen in the sample which will then form ash. The entire sample of the four variations of this process produces carbon sufficiently pure and can be seen in Table 1.

3.2 FTIR analysis

FTIR analysis is carried out to determine the available functional groups. The four main spectra generated from the wavelengths of 500 cm^{-1} to 4000 cm^{-1} are shown in Figure 1. The FTIR results of mango peel and activated mango peel in several variations. Overall, the results obtained have almost the same spectrum. The absorbance value of hydroxyl on the mango peel shows the number 3424 cm^{-1} . Other bonds in mango skin showed C=O stretching at 1739 cm^{-1} , and a wavelength at 1619 cm^{-1} indicates the presence of aromatic C=C absorption on the phenyl ring (Wang et al. 2012), C-H (stretch, symmetrical, asymmetrical) at 2924 cm^{-1} , and several other functional groups. In addition, there is also a carboxyl spectrum which is presented as deprotonated and allows bending of C-H bonds to form at a wavelength of 1380 cm^{-1} (Desalegnan et al. 2019). From several wave absorptions above, there is a wave disappearance in the activated mango peel. This disappearance occurs at a wave number of 1619 cm^{-1} (Rajeshkannan et al. 2011). The wave number indicates a stretched C=O hydroxyl bond (Iqbal et al. 2009). This stretching may be due to changes in counter ions associated with carboxylate and hydroxylate anions and suggests that carboxyl and hydroxyl groups are major contributors to metal ion absorption (Fiol et al. 2006).

TABLE 2. Equations of the Langmuir, Freundlich, and Dubinin-Radushkevich isotherm models.

Isotherm	Sample	General equation	Equation	R ²
Langmuir	a	$1/Q_e = 1/Q_0 + 1/Q_0 K_L C_e$	$1/Q_e = 0.164 + 0.1447/C_e$	0.9987
	b		$1/Q_e = 0.0348 + 0.1265/C_e$	0.9987
	c		$1/Q_e = 0.0498 + 0.1234/C_e$	0.9993
	d		$1/Q_e = 0.0318 + 0.1212/C_e$	0.9999
Freundlich	a	$\log Q_e = \log K_f + (1/n) \log C_e$	$\log Q_e = 0.4904 + 0.5853 \log C_e$	0.9959
	b		$\log Q_e = 0.8752 + 0.5495 \log C_e$	0.9765
	c		$\log Q_e = 0.8082 + 0.5696 \log C_e$	0.9928
	d		$\log Q_e = 0.9161 + 0.5635 \log C_e$	0.9856
Dubinin-Radushkevich	a	$\ln Q_e = \ln Q_m - K_{DR} \varepsilon^2$	$\ln Q_e = 1.4925 - 8.996510 - 8\varepsilon^2$	0.9788
	b		$\ln Q_e = 1.897 - 3.203510 - 8\varepsilon^2$	0.9983
	c		$\ln Q_e = 1.794 - 3.839710 - 8\varepsilon^2$	0.9918
	d		$\ln Q_e = 1.8676 - 3.009110 - 8\varepsilon^2$	0.9996

TABLE 3. Calculated parameter of each sample using adsorption Isotherm Model of Langmuir, Freundlich, and Dubinin-Raduskevich.

Sample name	L (R ²)	F (R ²)	D-R (R ²)	R _L (dimensionless)	Q _{max} (mg/g)	E (kJ/mol)
MPAC-1	0.9987	0.9959	0.9788	0.3617	6.9090	2.357
MPAC-2	0.9987	0.9765	0.9983	0.1208	7.9022	3.950
MPAC-3	0.9993	0.9928	0.9486	0.1678	8.1028	3.608
MPAC-4	0.9999	0.9856	0.9996	0.1160	8.2526	4.076

3.3 Adsorption modeling testing

The importance of the optimum contact time in influencing the maximum adsorption power of one absorbent. The two-hour contact time was chosen according to previous studies, which mention that the equilibrium condition reaches after 2 h (Abdel Salam et al. 2011). With this condition, we can model the isotherm according to Langmuir, Freundlich, and Dubinin-Radushkevich (D-R) isotherm.

Among the three adsorption isotherm models that have been presented in Figure 2 which is presented equation below in Table 2, the Langmuir isotherm model is the ideal one to use in the four sample variations. This is evidenced by the R² value which is close to one, which is worth 0.9987; 0.9987; 0.9993; and 0.9999. This shows that the monolayer adsorption process on Langmuir adsorbent has not been able to determine the adsorption mechanism.

Also accompanied by the variable R_L (separating factor/equilibrium factor) is shown by the following Equation 4.

$$\frac{1}{Q_e} = \frac{1}{Q_0} + \frac{1}{Q_0 K_L C_e} \tag{3}$$

$$R_L = \frac{1}{1 + K_L C_0} \tag{4}$$

where C₀ (mg / L) is the initial concentration and K_L (L / mg) is the Langmuir constant which corresponds to the adsorption energy. The results of the complete calculation of R_L,

TABLE 4. Percent Removal (%) obtained from each sample.

Sample name	Initial concentration (C ₀)	Equilibrium concentration (C _e)	% removal
MPAC-1	2	0.35	82.50
	4	0.93	76.75
	6	1.77	70.50
	7.77*	2.52	67.56
MPAC-2	2	0.09	95.50
	4	0.24	94.00
	6	0.60	90.00
	7.77*	1.22	84.29
MPAC-3	2	0.12	94.00
	4	0.34	91.50
	6	0.74	87.67
	7.77*	1.52	80.43
MPAC-4	2	0.08	96.00
	4	0.22	94.50
	6	0.52	91.33
	7.77*	1.18	84.81

Q_{max}, and Energy are shown in Table 3, with an explanation of the R_L values in the range 0 to 1 which indicates the isotherm form is unfavorable (R_L > 1), linear (R_L = 1), favorable (0 < R_L < 1) or irreversible (R_L = 0) (Meroufel et al., 2013). In this study, the R_L value was obtained from 0.11 to 0.36 (favorable), which means that the adsorption process went well. The R_L value is 0.11, so the MPAC-4 sample is considered to have a stronger bond to the Fe metal ion than the other three samples. Whereas in terms of Q_{max}, it can be seen that MPAC-4 has a maximum adsorption capacity of 8.25 mg / g which means it is greater than the variation of processes 1, 2, or 3. In addition, Langmuir's constant is obtained by relating the intercept and Q_{max} with values of 0.88; 3.63; 2.48; and 3.81.

Table 3 which shows the equation of the D-R line shows the variable E (energy) and the type of adsorption mechanism that occurs. The E (energy of D-R isotherm) number obtained in all samples is less than 8 kJ/mol, where this number shows that the adsorption mechanism that occurs is physical/physical adsorption (non-specific). Caused by the interaction between hydroxyl and carboxyl because the energy they have is not strong enough to cause chemical bonds. Physisorption occurs between the element carbon against the adsorbate (iron) and the element oxygen against the adsorbate (iron) due to differences in electronegativity. In addition, the high surface area due to the activation process that has been carried out provides an opportunity for the adsorbate to be absorbed (entrapment) so that Van der Waals forces occur more frequently. The physisorption that occurs is not too weak because the bond that occurs between the adsorbate and the adsorbent is only one layer (monolayer) so that the functional groups on the adsorbent are concentrated to bind to the adsorbate in a single layer.

3.4 Removal percentage

Overall, the process variation from MPAC-1 to MPAC-4 provides the percentage removal which continues to decrease as the initial ion concentration increases. This is all evidenced in the percent removal listed in Table 4. This condition shows that the ability of the adsorbent is not able to absorb the adsorbate in increasing abundance. The adsorbent will experience saturation in the adsorption process or in other words the adsorbent will no longer be able to absorb the adsorbate. The cause is the adsorbent pores that have been filled by the adsorbate (closed) so that the adsorbate is left in the solution around the adsorbent.

In the MPAC-1 sample (Table 4), the adsorption ability of Fe metal ions is the lowest compared to the other three samples. The reason is the activation process which only relies on physical activation so there are still many impurities in the skin of the mango fruit that is not dissolved by chemical agents. Meanwhile, MPAC-2 and MPAC-3 samples have

the adsorption ability exceed MPAC-1 samples due to the addition of functional groups during chemical activation with the emergence of new functional groups that will be needed during the adsorption process. However, MPAC-4 sample obtained the best percentage removal among the other three samples, namely 96%, 94.5%, 91.33%, and 84.81%, or in other words, it has the best adsorption ability of Fe ions. The reason is that when burning at 300 °C, some compounds decompose and are followed by chemical activation to clean impurities and clogged pores by utilizing the properties of the H₂SO₄ dehydrating agent. In addition, there is an activation process carried out when burning at 700 °C causes an increase in surface area with the complete decomposition of the compound. The more open pores will provide an opportunity for the adsorbate to diffuse into the adsorbent pores. This provides an opportunity for the adsorbent to interact with ion exchange and/or other interactions with metal ion Fe. The MPAC-4 adsorbent results indicate that the adsorption process of Fe metal ion in batik waste leaves 1.18 ppm, which can be categorized as environmentally friendly batik waste.

4. CONCLUSIONS

In this study, it can be concluded that activated mango peel (MP) can be used as an adsorbent to absorb Fe metal ions. Of the various processes tested, the MPAC-4 sample was the best process variation, with physical activation of 300 °C, followed by chemical activation, then physical activation of 700 °C, with the reason that the best removal percentages were 96%, 94.5%, 91.33%, and 84.81% for the initial Fe ion concentration 12, 4, 6, and batik waste, as evidenced by the absorption of Fe metal ions in batik waste that meets Ministry of Environment and Forestry standards, so that it can be disposed of to the environment, which is <5 ppm. Determination of the most appropriate isotherm model is the Langmuir isotherm model (monolayer) with physical adsorption mechanism.

5. NOTATION

List of notation:

C_0 = initial concentration of Fe²⁺ in solution, mg/L or ppm

C_A = final concentration of Fe²⁺ in solution, mg/L or ppm

V = volume of the solution, L

W = mass of the adsorbent, g

q_e = maximum adsorption capacity, mg/g

K_L = Langmuir constant

R_L = separation factor

ACKNOWLEDGMENTS

The author is grateful to all staff of the Chemical Engineering Laboratory of Universitas Pertamina who have helped the author by providing the opportunity to conduct research at the Chemical Engineering Laboratory, as well as all staff of the Badan Pengkajian dan Penerapan Teknologi (BPPT) who have assisted the author in obtaining sample analysis data.

REFERENCES

Abdel Salam OE, Reiad NA, ElShafei MM. 2011. A study of the removal characteristics of heavy metals from wastew-

ater by low-cost adsorbents. *Journal of Advanced Research*. 2(4):297–303. doi:<https://doi.org/10.1016/j.jare.2011.01.008>.

Ajmal M, Ali Khan Rao R, Anwar S, Ahmad J, Ahmad R. 2003. Adsorption studies on rice husk: removal and recovery of Cd(II) from wastewater. *Bioresource Technology*. 86(2):147–149. doi:[https://doi.org/10.1016/S0960-8524\(02\)00159-1](https://doi.org/10.1016/S0960-8524(02)00159-1).

Barakat MA. 2011. New trends in removing heavy metals from industrial wastewater. *Arabian Journal of Chemistry*. 4(4):361–377. doi:<https://doi.org/10.1016/j.arabjc.2010.07.019>.

Budiyanto S, Anies, Purnaweni H, Sunoko H. 2018. Environmental analysis of The impacts of batik waste water pollution on the quality of dug well water in the batik industrial center of Jenggot, Pekalongan city. *E3S Web of Conferences*. 31:9008. doi:[10.1051/e3sconf/20183109008](https://doi.org/10.1051/e3sconf/20183109008).

Correia LB, Fiuza RA, de Andrade RC, Andrade HMC. 2018. CO₂ capture on activated carbons derived from mango fruit (*Mangifera indica* L.) seed shells. *Journal of Thermal Analysis and Calorimetry*. 131(1):579–586. doi:[10.1007/s10973-017-6542-7](https://doi.org/10.1007/s10973-017-6542-7).

Desalegn B, Megharaj M, Chen Z, Naidu R. 2019. Green synthesis of zero valent iron nanoparticle using mango peel extract and surface characterization using XPS and GC-MS. *Heliyon*. 5(5):e01750. doi:<https://doi.org/10.1016/j.heliyon.2019.e01750>.

Fiol N, Villaescusa I, Martínez M, Miralles N, Poch J, Serarols J. 2006. Sorption of Pb(II), Ni(II), Cu(II) and Cd(II) from aqueous solution by olive stone waste. *Separation and Purification Technology*. 50(1):132–140. doi:<https://doi.org/10.1016/j.seppur.2005.11.016>.

Ghosh A, Chakravorty D, Rahaman M, Bose S. 2019. Efficiency of mango peel derived activated carbon prepared via different routes as adsorbent for rhodamine B BT. *Waste water recycling and management*. Singapore: Springer. p. 111–122. doi:[10.1007/978-981-13-2619-6_10](https://doi.org/10.1007/978-981-13-2619-6_10).

Gunatilake S. 2015. Methods of removing heavy metals from industrial wastewater. *Journal of Multidisciplinary Engineering Science Studies*. 1(1):12–18. <http://www.jmess.org/wp-content/uploads/2015/11/JMESSP13420004.pdf>.

Iqbal M, Saeed A, Zafar SI. 2009. FTIR spectrophotometry, kinetics and adsorption isotherms modeling, ion exchange, and EDX analysis for understanding the mechanism of Cd²⁺ and Pb²⁺ removal by mango peel waste. *Journal of Hazardous Materials*. 164(1):161–171. doi:[10.1016/j.jhazmat.2008.07.141](https://doi.org/10.1016/j.jhazmat.2008.07.141).

Kadirvelu K, Kavipriya M, Karthika C, Radhika M, Vennilamani N, Pattabhi S. 2003. Utilization of various agricultural wastes for activated carbon preparation and application for the removal of dyes and metal ions from aqueous solutions. *Bioresource Technology*. 87(1):129–132. doi:[10.1016/S0960-8524\(02\)00201-8](https://doi.org/10.1016/S0960-8524(02)00201-8).

Khan FSA, Mubarak NM, Tan YH, Karri RR, Khalid M, Walvekar R, Abdullah EC, Mazari SA, Nizamuddin S. 2020. Magnetic nanoparticles incorporation into different substrates for dyes and heavy metals removal—a review. *Environmental Science and Pollution Research*. 27(35):43526–43541. doi:[10.1007/s11356-020-10482-z](https://doi.org/10.1007/s11356-020-10482-z).

Mohan D, Singh KP. 2002. Single- and multi-component adsorption of cadmium and zinc using activated carbon de-

- rived from bagasse—an agricultural waste. *Water Research*. 36(9):2304–2318. doi:[10.1016/S0043-1354\(01\)00447-X](https://doi.org/10.1016/S0043-1354(01)00447-X).
- Orozco R, Hernández P, Morales G, Núñez FU, Villafuerte JO, Lugo VL, Ramírez N, Díaz C, Vázquez PC. 2014. Characterization of lignocellulosic fruit waste as an alternative feedstock for bioethanol production. *Bioresources*. 9:1873–1885. doi:[10.15376/biores.9.2.1873-1885](https://doi.org/10.15376/biores.9.2.1873-1885).
- Rajeshkannan R, Manivasagan R, Natarajan R. 2011. Decolourization of malachite green using tamarind seed: optimization, isotherm and kinetic studies. *Chemical Industry and Chemical Engineering Quarterly*. 17(1):67–79. doi:[10.2298/CICEQ100716056R](https://doi.org/10.2298/CICEQ100716056R).
- Sheth Y, Dharaskar S, Khalid M, Sonawane S. 2021. An environment friendly approach for heavy metal removal from industrial wastewater using chitosan based biosorbent: a review. *Sustainable Energy Technologies and Assessments*. 43:100951. doi:[10.1016/j.seta.2020.100951](https://doi.org/10.1016/j.seta.2020.100951).
- Tan WT, Ooi ST, Lee CK. 1993. Removal of chromium(VI) from solution by coconut husk and palm pressed fibres. *Environmental Technology*. 14(3):277–282. doi:[10.1080/09593339309385290](https://doi.org/10.1080/09593339309385290).
- Wang Z, Nie E, Li J, Yang M, Zhao Y, Luo X, Zheng Z. 2012. Equilibrium and kinetics of adsorption of phosphate onto iron-doped activated carbon. *Environmental Science and Pollution Research*. 19(7):2908–2917. doi:[10.1007/s11356-012-0799-y](https://doi.org/10.1007/s11356-012-0799-y).